Ultrarelativistic Electron-Beam Polarization in Single-Shot Interaction with an Ultraintense Laser Pulse

Yan-Fei Li,[1] Rashid Shaisultanov,[2] Karen Z. Hatsagortsyan,[2,*] Feng Wan,[1]
Christoph H. Keitel,[2] and Jian-Xing Li[1,†]
[1]*MOE Key Laboratory for Nonequilibrium Synthesis and Modulation of Condensed Matter, School of Science, Xi'an Jiaotong University, Xi'an 710049, China*
[2]*Max-Planck-Institut für Kernphysik, Saupfercheckweg 1, 69117 Heidelberg, Germany*

(Received 18 December 2018; published 19 April 2019)

Spin polarization of an ultrarelativistic electron beam head-on colliding with an ultraintense laser pulse is investigated in the quantum radiation-dominated regime. We develop a Monte Carlo method to model electron radiative spin effects in arbitrary electromagnetic fields by employing spin-resolved radiation probabilities in the local constant field approximation. Because of spin-dependent radiation reaction, the applied elliptically polarized laser pulse polarizes the initially unpolarized electron beam and splits it along the propagation direction into two oppositely transversely polarized parts with a splitting angle of about tens of milliradians. Thus, a dense electron beam with above 70% polarization can be generated in tens of femtoseconds with realistic laser pulses. The proposed method demonstrates a way for relativistic electron beam polarization with currently achievable laser facilities.

DOI: 10.1103/PhysRevLett.122.154801

Spin-polarized electron beams are extensively employed to investigate matter properties, atomic and molecular structures [1–3], and in the relativistic realm, probe nuclear structures [4,5], generate polarized photons [6,7] and positrons [6,8], study parity violation [9] and new physics beyond the standard model [10]. There are mainly two methods to generate relativistic polarized electron beams [11]. In the first method, the polarized electrons are first extracted from a photocathode [12,13] and then, accelerated (alternatively obtained from spin filters [14], beam splitters [15,16], or laser wakefield acceleration in prepolarized plasmas [17]). The second method is a direct way of transverse polarization of a relativistic electron beam in a storage ring via radiative polarization (Sokolov-Ternov effect) [18–25]. The polarization of the latter is rather slow, because the magnetic fields of a synchrotron are too weak (∼1 Tesla). Because mostly longitudinal polarization is interesting in high-energy physics, spin rotation systems are applied [26]. Moreover, for creating polarized positrons, Compton scattering or Bremsstrahlung of circularly polarized lasers and successive pair creation are commonly used [27–31]. The polarization of relativistic electrons can be detected by Compton scattering [32], Møller scattering [33], or other methods.

Strongest fields in a laboratory are provided by lasers, reaching a laser intensity $\sim 10^{22}$ W/cm^2 (magnetic field $\sim 4\times 10^5$ Tesla) [34–37]. Can such strong fields be employed for fast electron polarization, similar to the Sokolov-Ternov effect? Unfortunately, previous investigations proved that electrons cannot be polarized via asymmetric spin flip in nonlinear Compton scattering off a strong monochromatic plane laser wave [38–41], because of the oscillating character of laser fields, with opposite directions of the magnetic field in adjacent half cycles. For the same reason the polarization is small in the case of a laser pulse [42–44]. In a plane-wave ultrashort laser pulse, 9% degree of electron polarization has been recently shown in Ref. [44]. It is also known that because of linear Compton scattering the electrons of different spins are scattered off the beam with different probabilities, and the unscattered part of the beam becomes polarized [45]; however, the number of electrons
in the beam is significantly decreased. Therefore, it still remains a challenge to obtain a significant polarization of an electron beam in realistic space-time oscillating laser fields. In this respect, recently a model electromagnetic field, namely, a strong rotating electric field has been shown to highly polarize an electron beam analogous to the Sokolov-Ternov effect in tens of femtoseconds [46,47]. The rotating electric field models antinodes of the electric field of a standing laser wave. However, it is known that at available strong laser intensities the electrons are mostly trapped at nodes of the electric field, rather than antinodes [48,49], while the radiative trapping in antinodes may only occur in future linearly polarized laser pulses of intensities $\gtrsim 10^{26}$ W/cm^2 [50].

In this Letter, we show that with a proper choice of ellipticity of a currently achievable strong laser pulse interacting with a counterpropagating unpolarized electron beam in the quantum radiation-dominated regime [51], the

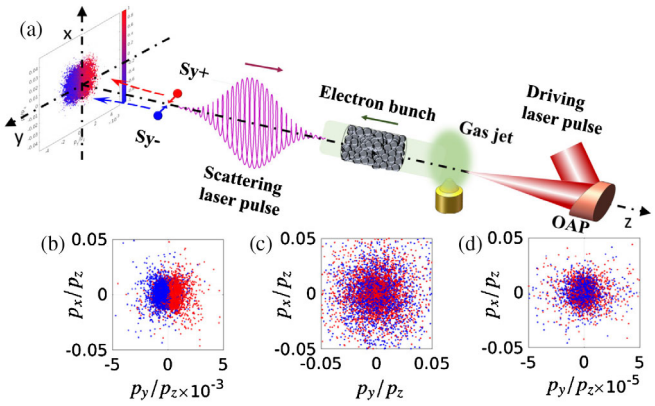

FIG. 1. Scenario of generation of spin-polarized electron beams via nonlinear Compton scattering. (a) An ultrarelativistic electron bunch generated by laser wakefield acceleration collides head-on with an ultraintense elliptically polarized laser pulse. "S_{y+}" (red point) and "S_{y-}" (blue point) denote the electrons polarized parallel and antiparallel to the y direction, respectively. Transverse momentum distributions: for (b) EP, (c) CP, and (d) LP laser pulses. The laser pulse propagates along $+z$ direction, and the major axis of the polarization ellipse is along x axis.

electron beam can be polarized and splitted along the propagation direction into two parts with opposite transverse polarizations (see Fig. 1). The electron beam splitting is due to spin-dependent radiation reaction. It is interesting to note that the considered effect is damped in the circularly polarized (CP) and linearly polarized (LP) laser fields, but is significant in the elliptically polarized (EP) one with a proper ellipticity; see Figs. 1(b) and 1(d) and the detailed explanation below in Fig. 3. For the analysis of radiative spin effects, we have developed a Monte Carlo method for photon emissions during the electron semiclassical dynamics in external laser field, which is based on the spin-resolved radiation probability in the local constant field approximation (LCFA) [52–62].

In nonlinear Compton scattering, the invariant parameter characterizing quantum effects is $\chi \equiv |e|\hbar\sqrt{(F_{\mu\nu}p^{\nu})^2}/m^3c^4$ [52], where $F_{\mu\nu}$ is the field tensor, $\hbar$ the reduced Planck constant, c the speed of the light, $p = (\varepsilon/c, \mathbf{p})$ the incoming electron 4-momentum, and $-e$ and m are the electron charge and mass, respectively. When the electron counterpropagates with the laser beam, $\chi \approx 2(\hbar\omega_0/mc^2)\xi\gamma$. Here, γ is the electron Lorentz factor, $\xi \equiv |e|E_0/(m\omega_0 c)$ the invariant laser field parameter, E_0 and ω_0 are the amplitude and frequency of the laser field, respectively.

We simulate spin-resolved electron dynamics with a Monte Carlo code. Photon emissions are treated quantum mechanically in LCFA valid at $\xi \gg 1$ [52,53,63]. The spin-dependent photon emission probabilities in LCFA are employed with the leading order contribution with respect to $1/\gamma$, which are derived with the quantum electrodynamics operator method of Baier-Katkov [64]

$$\begin{aligned}\frac{d^2W_{fi}}{dud\eta} = W_R\{&-(2+u)^2[\mathrm{Int}K_{\frac{1}{3}}(u') - 2K_{\frac{2}{3}}(u')](1+\mathbf{S}_{if})\\ &+u^2[\mathrm{Int}K_{\frac{1}{3}}(u') + 2K_{\frac{2}{3}}(u')](1-\mathbf{S}_{if}) + 2u^2\mathbf{S}_{if}\mathrm{Int}K_{\frac{1}{3}}(u')\\ &-(4u+2u^2)(\mathbf{S}_f+\mathbf{S}_i)[\boldsymbol{\beta}\times\hat{\mathbf{a}}]K_{\frac{1}{3}}(u')\\ &-2u^2(\mathbf{S}_f-\mathbf{S}_i)[\boldsymbol{\beta}\times\hat{\mathbf{a}}]K_{\frac{1}{3}}(u')\\ &-4u^2[\mathrm{Int}K_{\frac{1}{3}}(u') - K_{\frac{2}{3}}(u')](\mathbf{S}_i\cdot\boldsymbol{\beta})(\mathbf{S}_f\cdot\boldsymbol{\beta})\}, \end{aligned} \tag{1}$$

where $W_R = \alpha mc/[8\sqrt{3}\pi\lambda\!\!\!^{-}_c(k\cdot p_i)(1+u)^3]$, $u' = 2u/3\chi$, $u = \hbar\omega_\gamma/(\varepsilon_i - \hbar\omega_\gamma)$, $\mathrm{Int}K_{\frac{1}{3}}(u') \equiv \int_{u'}^{\infty} dz K_{\frac{1}{3}}(z)$, K_n is the n-order modified Bessel function of the second kind, α the fine structure constant, $\lambda\!\!\!^{-}_c = \hbar/mc$ the Compton wavelength, ω_γ the emitted photon frequency, ε_i the electron energy before radiation, $\boldsymbol{\beta} = \mathbf{v}/c$ the velocity, $\hat{\mathbf{a}} = \mathbf{a}/|\mathbf{a}|$ the acceleration, $\eta = k\cdot r$ the laser phase, p_i, k, and r are four vectors of the electron momentum before radiation, laser wave vector, and coordinate, respectively, $\mathbf{S}_i$ and $\mathbf{S}_f$ denote the electron spin polarization vector before and after radiation, respectively, $|\mathbf{S}_{i,f}| = 1$, and $\mathbf{S}_{if} \equiv \mathbf{S}_i\cdot\mathbf{S}_f$. The case when $\mathbf{S}_i$ and $\mathbf{S}_f$ are along the magnetic field in the rest frame of electron is given in Ref. [65]. Arbitrary spin directions are necessary in Eq. (1) to consistently include in the Monte Carlo code the electron spin precession effect in the laser field between the photon emissions. Summing over $\mathbf{S}_f$, the radiation probability depending on the initial spin is obtained [64]

$$\begin{aligned}\frac{d^2\bar{W}_{fi}}{dud\eta} = 8W_R\{&-(1+u)\mathrm{Int}K_{\frac{1}{3}}(u') + (2+2u+u^2)K_{\frac{2}{3}}(u')\\ &- u\mathbf{S}_i\cdot[\boldsymbol{\beta}\times\hat{\mathbf{a}}]K_{\frac{1}{3}}(u')\}. \end{aligned} \tag{2}$$

Averaging by the electron initial spin, the widely used radiation probability is obtained [55–59]. The radiation probabilities in Eqs. (1) and (2) are summed up by photon polarization.

The spin dynamics due to photon emissions are described in the spirit of the quantum jump approach [66,67]. After a photon emission, the electron spin state is collapsed into one of its basis states defined with respect to the instantaneous spin quantization axis (SQA), which is chosen along the magnetic field in the rest frame of electron, i.e., along $\boldsymbol{\beta}\times\hat{\mathbf{a}}$. We consider the stochastic spin flip at photon emission using three random numbers N_r, N_r', and N_r'' in [0, 1], as follows. First, at each emission length, because the spin-dependent radiation probability in Eq. (2) $\bar{W}_{fi} \geq N_r$, a photon is emitted. The emitted photon frequency ω_γ is determined by the condition $(1/\bar{W}_{fi})\int_{\omega_0}^{\omega_\gamma}\{[d\bar{W}_{fi}(\omega)]/(d\omega)\}d\omega = N_r'$. Then, the electron spin flips either parallel (spin-up) or antiparallel (spin-down) to SQA with probabilities of $W_{fi}^{\uparrow}$ and $W_{fi}^{\downarrow}$, respectively. Here, $\bar{W}_{fi} = W_{fi}^{\uparrow} + W_{fi}^{\downarrow}$ and $W_{fi}^{\uparrow}$ and

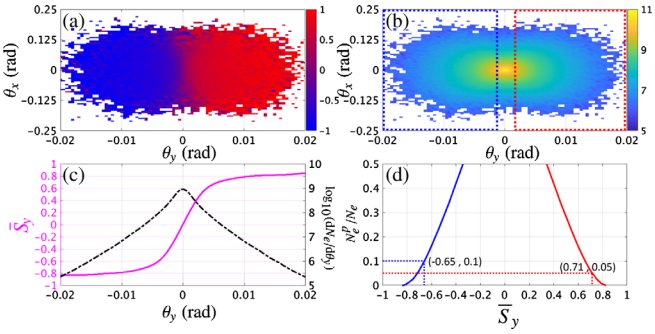

FIG. 2. (a) Transverse distribution of the electron spin component S_y vs the deflection angles $\theta_x = \arctan(p_x/p_z)$ and $\theta_y = \arctan(p_y/p_z)$. (b) Transverse distribution of the electron density $\log_{10}(\mathrm{d}^2N_e/\mathrm{d}\theta_x\mathrm{d}\theta_y)$ rad^{-2}. (c) Average spin $\bar{S}_y$ (magenta solid) and electron distribution $\log_{10}(\mathrm{d}N_e/\mathrm{d}\theta_y)$ (black dashed) vs θ_y. (d) Ratio of polarized electron number N_e^p to total electron number N_e vs the beam average spin $\bar{S}_y$. The red (right) and blue (left) curves represent the polarization parallel and antiparallel to the $+y$ axis, respectively. And, the points $(-0.65, 0.1)$ and $(0.71, 0.05)$ indicate $(\bar{S}_y, N_e^p/N_e)$ of electrons in the blue and red boxes in panel (b), respectively. The laser and electron beam parameters are given in the text.

$W_{fi}^{\downarrow}$ are calculated via Eq. (1). If $W_{fi}^{\uparrow}/\bar{W}_{fi} \geq N_r''$, the spin flips up, otherwise, down.

Between photon emissions, the electron dynamics in the external laser field is described by Lorentz equations, and the spin precession is governed by the Thomas-Bargmann-Michel-Telegdi equation [68–71]:

$$\frac{d\mathbf{S}}{d\eta} = \frac{e\gamma}{c(k\cdot p)}\mathbf{S}\times\left[-\left(\frac{g}{2}-1\right)\frac{\gamma}{\gamma+1}(\boldsymbol{\beta}\cdot\mathbf{B})\boldsymbol{\beta} + \left(\frac{g}{2}-1+\frac{1}{\gamma}\right)\mathbf{B} - \left(\frac{g}{2}-\frac{\gamma}{\gamma+1}\right)\boldsymbol{\beta}\times\mathbf{E}\right], \quad (3)$$

where $\mathbf{E}$ and $\mathbf{B}$ are the laser electric and magnetic fields, respectively, g is the electron gyromagnetic factor [21]: $g(\chi) = 2+2\mu(\chi)$, $\mu(\chi) = [\alpha/(\pi\chi)]\int_0^\infty [y/(1+y)^3]\mathbf{L}_{\frac{1}{3}}[(2y)/(3\chi)]dy$, with $\mathbf{L}_{\frac{1}{3}}(z) = \int_0^\infty \sin\{[(3z)/2][x+(x^3/3)]\}dx$. Because $\chi \ll 1$, $g \approx 2.00232$. The accuracy of our Monte Carlo code is confirmed by reproducing the well-known results on the radiative polarization [19,21,46,47,72].

The spatial distribution of the electromagnetic fields takes into account up to $(w_0/z_r)^3$ order of the nonparaxial solution [72–74], where w_0 is the laser beam waist and z_r the Rayleigh length.

The considered polarization effect is illustrated in Fig. 2. The laser peak intensity $I_0 \approx 1.38\times10^{22}$ W/cm^2 ($\xi = 100$), wavelength $\lambda_0 = 1$ μm, pulse duration $\tau = 5T_0$ with period T_0, focal radius $w_0 = 5$ μm, and ellipticity $\epsilon = |E_y|/|E_x| = 0.05$. For the cylindrical electron bunch, polar angle $\theta_e = 180°$, azimuthal angle $\phi_e = 0°$, and angular divergence is 0.3 mrad. Initial kinetic energy $\epsilon_0 =$ 4 GeV with an energy spread $\Delta\epsilon_0/\epsilon_0 = 0.06$, $\chi_{\max} \approx 1.5$

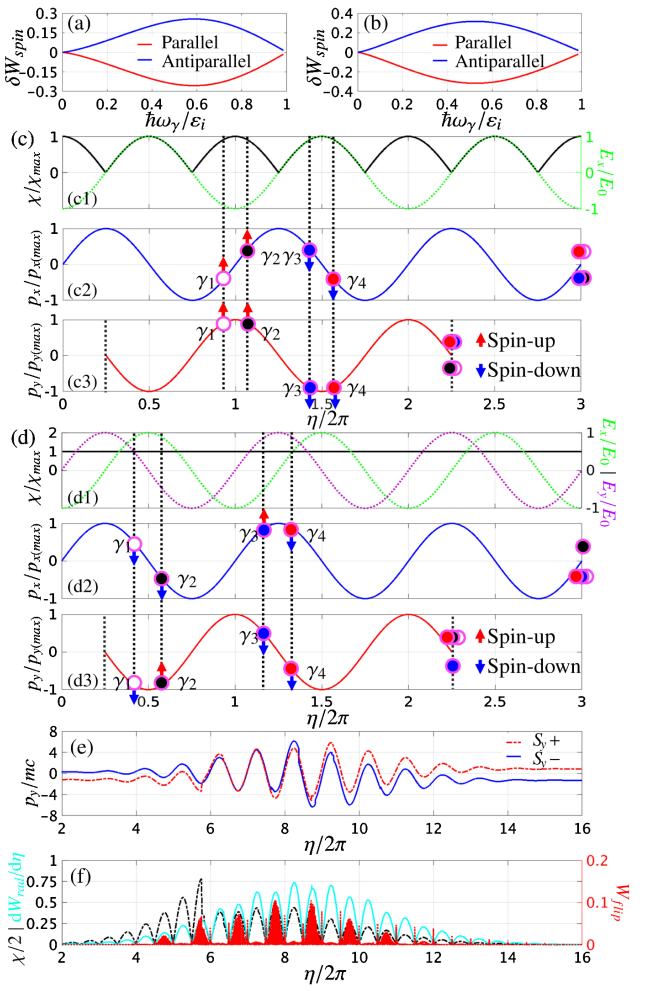

FIG. 3. (a), (b): The relative magnitude of the spin-dependent term in the radiation probability of Eq. (2) with $\chi = 1$ and 0.1, respectively. $\delta W_{\mathrm{spin}} \equiv W_{\mathrm{spin}}/(W_{\mathrm{rad}} - W_{\mathrm{spin}})$, and, W_{rad} and W_{spin} are the total radiation probability and the spin-dependent term in Eq. (2), respectively. Red and blue curves denote $\mathbf{S}_i$ parallel and antiparallel to SQA, respectively. (c),(d): Electron momenta in EP (LP) and CP plane waves, respectively. The colored circles indicate the photon emission points in the laser field and the corresponding electron final momenta. The red-up (blue-down) arrows indicate "spin-up" ("spin-down") with respect to $+y$ axis in (c2), (c3), and (d2), and $+x$ axis in (d3). (e) Scaled p_y of two sample electrons vs η. (f) Scaled χ (black), radiation probability W_{rad} (cyan) and flip probability W_{flip} (red) vs η for a sample electron. The laser and electron beam parameters in (e) and (f) are the same as in Fig. 2.

(the pair production is estimated to be negligible for present parameters). The bunch radius $w_e = \lambda_0$, length $L_e = 5\lambda_0$, and density $n_e \approx 2.6\times10^{17}$ cm^{-3} with a transversely Gaussian and longitudinally uniform distribution, which can be obtained by current laser wakefield accelerators [75,76]. The feasibility of elliptical polarization of ultrastrong laser beams is demonstrated in Refs. [77,78].

Figure 2(a) demonstrates that an initially unpolarized electron bunch is polarized and splitted into two beams

polarizing parallel and antiparallel to the minor axis of elliptical polarization ($+y$ axis), respectively, with a splitting angle of about 20 mrad, which is much larger than the angular divergence of the electron beams [72]. The corresponding electron density mainly concentrates in the beam center, because the transverse ponderomotive force is relatively small; see Fig. 2(b). Figure 2(c) represents the average spin $\bar{S}_y$ (magenta-solid curve) and the electron density distribution (black-dashed curve) integrated over θ_x. Near $\theta_y = 0$, the electron density is rather high, but $\bar{S}_y$ is very low. With the increase of $|\theta_y|$, the electron density exponentially declines; however, $\bar{S}_y$ remarkably ascends until about 80%. Separating the part of the electron beam within $\theta_y > 0$ (or $\theta_y < 0$), one will obtain an electron beam with positive (or negative) transverse polarization. When splitting the beams exactly at $\theta_y = 0$, one obtains $|\bar{S}_y| \approx 34.21\%$ for both the splitted beams. However, we can increase the polarization of beams if we exclude the electrons near $\theta_y = 0$. For instance, as is shown by blue and red boxes in Fig. 2(b), the corresponding average spin $\bar{S}_y$ and electron number ratio N_e^p/N_e are approximately $(-65\%, 10\%)$ and $(71\%, 5\%)$, respectively, see Fig. 2(d). The corresponding splitting angle is of about 3 mrad, which is much larger than the angular resolution (less than 0.1 mrad) with current technique of electron detectors [76,79–81].

Moreover, for experimental convenience, we consider the cases of larger energy spread $\Delta\varepsilon_0/\varepsilon_0 = 0.1$, larger angular divergence of 1 mrad and different collision angles $\theta_e = 179°$ and $\phi_e = 90°$, and all show stable and uniform results [72].

The reason for the electron beam polarization and splitting is analyzed in Fig. 3. The spin effect in the radiation probability is due to the third term in Eq. (2), and its contribution is rather significant (about 30%) for high-energy photon emission; see Figs. 3(a) and 3(b) at $\hbar\omega_\gamma/\varepsilon_i \approx 0.5 \sim 0.6$, which is negative (positive) for $\mathbf{S}_i$ parallel (antiparallel) to SQA. For simplicity, we analyze the electron radiative dynamics in plane wave cases; see Figs. 3(c) and 3(d). Let us assume that the relativistic electrons initially move along $-z$ direction, have no transverse momentum, and the final polarization along y axis is detected. When in the laser field the electron emits a photon (mostly at large χ) with a transverse momentum, finally it will appear with an opposite one due to the momentum conservation. The ultrarelativistic electron is assumed to emit a photon along its momentum direction, because the emission angle $\sim 1/\gamma$ is rather small. Therefore, the electron final transverse momentum will be opposite in sign to its momentum at the photon emission point. In the laser field the transverse momentum $\mathbf{p}_\perp = -e\mathbf{A}(\eta)$, with the vector potential $\mathbf{A}(\eta)$, is ahead by $\pi/2$ with respect to the field $\mathbf{E}(\eta)$. The SQA is along $\boldsymbol{\beta} \times \hat{\mathbf{a}} \propto e\boldsymbol{\beta} \times \mathbf{E} + e\boldsymbol{\beta} \times (\boldsymbol{\beta} \times \mathbf{B}) \sim e(1 - \boldsymbol{\beta}_z)\boldsymbol{\beta} \times \mathbf{E}$, and note that $\boldsymbol{\beta}$ is negative.

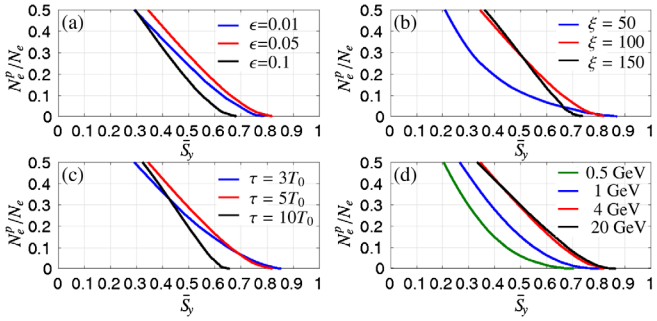

FIG. 4. Impacts of (a) ellipticity ϵ, (b) laser intensity ξ, (c) laser pulse duration τ, and (d) initial kinetic energy of electrons ε_0 on the polarization. Other parameters are the same as in Fig. 2.

For the LP plane wave polarized along x axis, see Figs. 3(c1)and 3(c2), $\chi \propto \xi\gamma$ oscillates with $|E_x|$, and the SQA is along y axis, with a sign following E_x. According to Eq. (2) and Figs. 3(a) and 3(b), at points of γ_1, γ_2, the photon emission is more probable for spin-up (with respect to $+y$ direction) electrons, because the corresponding E_x (green curve), and consequently, SQA are both negative. At points of γ_3 and γ_4, spin-down electrons mostly radiate. The final transverse momenta of electrons emitting photons at γ_1 and γ_4 are positive and at γ_2 and γ_3 negative. Consequently, spin-up and spin-down electrons move symmetrically with respect to the x axis and mix together, as indicated in Fig. 1(d). The similar analysis is applicable for the CP case; see Figs. 3(d1)–3(d3). Finally, spin-up and spin-down electrons mix together in x-y plane; see Fig. 1(c).

However, for the EP plane wave with a rather small ellipticity ($E_y \ll E_x$), the radiation probability and the SQA both mainly rely on E_x, and the SQA is along y axis. In Fig. 3(c3), p_y has a π delay with respect to E_x; at points of γ_1 and γ_2, E_x and SQA are both negative, thus, spin-up (with respect to $+y$ direction) electrons more probably radiate and finally acquire negative p_y. And, at points of γ_3 and γ_4, spin-down electrons more probably radiate and finally have positive p_y. Consequently, electrons split up with respect to the $+y$ axis; see Figs. 1(b) and 2, in which, because p_z is negative, spin-up (spin-down) electrons move at positive (negative) $\theta_y = \arctan(p_y/p_z)$. The trajectories of sample electrons in Fig. 3(e) illustrate those behaviors.

We underline that the spin-dependent beam splitting relies on the spin-dependent radiation reaction, rather than on the asymmetric spin flip. Moreover, multiple flips of spin will smear out the considered effect, and we judiciously have chosen parameters to reduce the flip effect via limiting the number of emitted photons $N_{\rm ph} \sim \xi\alpha\tau/T_0 \approx 3.65$ [51,72], along with rather small spin flip probability; see Fig. 3(f).

Furthermore, impacts of the laser and electron beam parameters on the polarization are analyzed in Fig. 4. First, the ellipticity ϵ is a very crucial parameter. If ϵ is too small,

the splitting angle $\theta_s \sim p_y/p_x \propto E_y/E_x$ is very small as well, and the polarized electrons partially overlap near $p_y = 0$ (e.g., the ultimate case of the LP laser), which reduces the degree of polarization. Oppositely, largely increasing ellipticity can increase the splitting angle, but unfortunately also the SQA rotation (cf., the ultimate case of the CP laser). Thus, the average polarization decreases; see Fig. 4(a). The optimal ellipticity is of order of 10^{-2} to 10^{-1}. The trade-off exists also for the laser intensity, pulse duration, and the electron energy. From one side, the effect relies on the radiation reaction and requires large $\chi \approx 10^{-6}\xi\gamma \gtrsim 1$ and many photon emissions. From another side, the spin flips smear out the considered effect which imposes restriction on the photon emissions. For this reason, with increasing ξ and the electron kinetic energy ε_0, the polarization is first enhanced due to the increase of χ, and then saturates; see Figs. 4(b) and 4(d). The mentioned trade-off yields nonuniform dependence on the laser pulse duration. The polarization is weak at too short or too long pulses, and the optimum is $\tau = 5T_0$ for the given parameters; see Fig. 4(c).

For a simple estimation of radiative polarization effects, we also develop a semiclassical analytical method based on the modified Landau-Lifshitz equation [51,82,83] with a radiation-reaction force accounting for quantum-recoil and spin effects. This model further confirms above obtained results qualitatively [72].

In conclusion, we have developed a Monte Carlo method for simulating radiative spin effects. We show that adding a proper small ellipticity to the strong laser pulse allows us to directly polarize and split a counterpropagating relativistic electron beam into highly polarized parts with current achievable experimental techniques, which can be used in high-energy physics.

We are grateful to A. Di Piazza and M. Tamburini for helpful discussions. This work is supported by the National Natural Science Foundation of China (Grants No. 11874295 and No. 11804269), the Science Challenge Project of China (Grant No. TZ2016099), and the National Key Research and Development Program of China (Grant No. 2018YFA0404801).

*k.hatsagortsyan@mpi-hd.mpg.de
†jianxing@xjtu.edu.cn

[1] J. Kessler, *Polarized Electrons* (Springer, Berlin, 1985).
[2] M. Getzlaff, *Surface Magnetism* (Springer, Berlin, 2010).
[3] T. Gay, Adv. At. Mol. Opt. Phys. **57**, 157 (2009).
[4] K. Abe *et al.*, Phys. Rev. Lett. **75**, 25 (1995).
[5] V. Alexakhin *et al.*, Phys. Lett. B **647**, 8 (2007).
[6] H. Olsen and L. C. Maximon, Phys. Rev. **114**, 887 (1959).
[7] R. Märtin, G. Weber, R. Barday, Y. Fritzsche, U. Spillmann, W. Chen, R. D. DuBois, J. Enders, M. Hegewald, S. Hess, A. Surzhykov, D. B. Thorn, S. Trotsenko, M. Wagner, D. F. A. Winters, V. A. Yerokhin, and T. Stöhlker, Phys. Rev. Lett. **108**, 264801 (2012).
[8] D. Abbott *et al.* (PEPPo Collaboration), Phys. Rev. Lett. **116**, 214801 (2016).
[9] P. L. Anthony *et al.* (SLAC E158 Collaboration), Phys. Rev. Lett. **92**, 181602 (2004).
[10] G. Moortgat-Pick *et al.*, Phys. Rep. **460**, 131 (2008).
[11] M. L. Swartz, Physics with Polarized Beams, Report No. SLAC-PUB-4656 (1988).
[12] D. T. Pierce and F. Meier, Phys. Rev. B **13**, 5484 (1976).
[13] D. T. Pierce, F. Meier, and P. Zürcher, Appl. Phys. Lett. **26**, 670 (1975).
[14] H. Batelaan, A. S. Green, B. A. Hitt, and T. J. Gay, Phys. Rev. Lett. **82**, 4216 (1999).
[15] M. M. Dellweg and C. Müller, Phys. Rev. Lett. **118**, 070403 (2017).
[16] M. M. Dellweg and C. Müller, Phys. Rev. A **95**, 042124 (2017).
[17] M. Wen, M. Tamburini, and C. H. Keitel, arXiv:1809.10570.
[18] A. A. Sokolov and I. M. Ternov, Sov. Phys. Dokl. **8**, 1203 (1964).
[19] A. A. Sokolov and I. M. Ternov, *Synchrotron Radiation* (Akademic, Germany, 1968).
[20] V. Baier and V. Katkov, Phys. Lett. A **24**, 327 (1967).
[21] V. N. Baier, Sov. Phys. Usp. **14**, 695 (1972).
[22] Y. Derbenev and A. M. Kondratenko, Zh. Èksper. Teoret. Fiz. **64**, 1918 (1973) [Sov. Phys. JETP **37**, 968 (1973)].
[23] V. N. Baier, V. M. Katkov, and V. M. Strakhovenko, Phys. Lett. B **70**, 83 (1977).
[24] Y. S. Derbenev, A. M. Kondratenko, and A. N. Skrinsky, Part. Accel. **9**, 247 (1979).
[25] S. R. Mane, Phys. Rev. A **36**, 105 (1987).
[26] J. Buon and K. Steffen, Nucl. Instrum. Methods Phys. Res., Sect. A **245**, 248 (1986).
[27] T. Hirose, K. Dobashi, Y. Kurihara, T. Muto, T. Omori, T. Okugi, I. Sakai, J. Urakawa, and M. Washio, Nucl. Instrum. Methods Phys. Res., Sect. A **455**, 15 (2000).
[28] T. Omori, M. Fukuda, T. Hirose, Y. Kurihara, R. Kuroda, M. Nomura, A. Ohashi, T. Okugi, K. Sakaue, T. Saito, J. Urakawa, M. Washio, and I. Yamazaki, Phys. Rev. Lett. **96**, 114801 (2006).
[29] X. Artru, R. Chehab, M. Chevallier, V. Strakhovenko, A. Variola, and A. Vivoli, Nucl. Instrum. Methods Phys. Res., Sect. B **266**, 3868 (2008).
[30] T.-O. Müller and C. Müller, Phys. Lett. B **696**, 201 (2011).
[31] A. Di Piazza, A. I. Milstein, and C. Müller, Phys. Rev. A **82**, 062110 (2010).
[32] D. Barber *et al.*, Nucl. Instrum. Methods Phys. Res., Sect. A **329**, 79 (1993).
[33] P. S. Cooper, M. J. Alguard, R. D. Ehrlich, V. W. Hughes, H. Kobayakawa, J. S. Ladish, M. S. Lubell, N. Sasao, K. P. Schüler, P. A. Souder, G. Baum, W. Raith, K. Kondo, D. H. Coward, R. H. Miller, C. Y. Prescott, D. J. Sherden, and C. K. Sinclair, Phys. Rev. Lett. **34**, 1589 (1975).
[34] The Vulcan facility, http://www.clf.stfc.ac.uk/Pages/The-Vulcan-10-Petawatt-Project.aspx.
[35] The Extreme Light Infrastructure (ELI), http://www.eli-beams.eu/en/facility/lasers/.
[36] Exawatt Center for Extreme Light Studies (XCELS), http://www.xcels.iapras.ru/.

[37] V. Yanovsky, V. Chvykov, G. Kalinchenko, P. Rousseau, T. Planchon, T. Matsuoka, A. Maksimchuk, J. Nees, G. Cheriaux, G. Mourou, and K. Krushelnick, Opt. Express **16**, 2109 (2008).

[38] P. Panek, J. Z. Kamiński, and F. Ehlotzky, Phys. Rev. A **65**, 022712 (2002).

[39] G. L. Kotkin, V. G. Serbo, and V. I. Telnov, Phys. Rev. ST Accel. Beams **6**, 011001 (2003).

[40] D. Y. Ivanov, G. L. Kotkin, and V. G. Serbo, Eur. Phys. J. C **36**, 127 (2004).

[41] D. V. Karlovets, Phys. Rev. A **84**, 062116 (2011).

[42] M. Boca, V. Dinu, and V. Florescu, Nucl. Instrum. Methods Phys. Res., Sect. B **279**, 12 (2012).

[43] K. Krajewska and J. Z. Kamiński, Laser Part. Beams **31**, 503 (2013).

[44] D. Seipt, D. Del Sorbo, C. P. Ridgers, and A. G. R. Thomas, Phys. Rev. A **98**, 023417 (2018).

[45] Y. S. Derbenev, A. M. Kondratenko, and E. L. Saldin, Nucl. Instrum. Methods **165**, 15 (1979).

[46] D. Del Sorbo, D. Seipt, T. G. Blackburn, A. G. R. Thomas, C. D. Murphy, J. G. Kirk, and C. P. Ridgers, Phys. Rev. A **96**, 043407 (2017).

[47] D. Del Sorbo, D. Seipt, A. G. R. Thomas, and C. P. Ridgers, Plasma Phys. Controlled Fusion **60**, 064003 (2018).

[48] G. Lehmann and K. H. Spatschek, Phys. Rev. E **85**, 056412 (2012).

[49] J. G. Kirk, Plasma Phys. Controlled Fusion **58**, 085005 (2016).

[50] A. Gonoskov, A. Bashinov, I. Gonoskov, C. Harvey, A. Ilderton, A. Kim, M. Marklund, G. Mourou, and A. Sergeev, Phys. Rev. Lett. **113**, 014801 (2014).

[51] A. Di Piazza, C. Müller, K. Z. Hatsagortsyan, and C. H. Keitel, Rev. Mod. Phys. **84**, 1177 (2012).

[52] V. I. Ritus, J. Sov. Laser Res. **6**, 497 (1985).

[53] V. N. Baier, V. M. Katkov, and V. M. Strakhovenko, *Electromagnetic Processes at High Energies in Oriented Single Crystals* (World Scientific, Singapore, 1998).

[54] M. K. Khokonov and H. Nitta, Phys. Rev. Lett. **89**, 094801 (2002).

[55] I. V. Sokolov, J. A. Nees, V. P. Yanovsky, N. M. Naumova, and G. A. Mourou, Phys. Rev. E **81**, 036412 (2010).

[56] N. V. Elkina, A. M. Fedotov, I. Y. Kostyukov, M. V. Legkov, N. B. Narozhny, E. N. Nerush, and H. Ruhl, Phys. Rev. ST Accel. Beams **14**, 054401 (2011).

[57] C. Ridgers, J. Kirk, R. Duclous, T. Blackburn, C. Brady, K. Bennett, T. Arber, and A. Bell, J. Comput. Phys. **260**, 273 (2014).

[58] D. Green and C. Harvey, Comput. Phys. Commun. **192**, 313 (2015).

[59] C. N. Harvey, A. Ilderton, and B. King, Phys. Rev. A **91**, 013822 (2015).

[60] A. Di Piazza, M. Tamburini, S. Meuren, and C. H. Keitel, Phys. Rev. A **98**, 012134 (2018).

[61] A. Ilderton, B. King, and D. Seipt, arXiv:1808.10339.

[62] A. Di Piazza, M. Tamburini, S. Meuren, and C. H. Keitel, Phys. Rev. A **99**, 022125 (2019).

[63] M. K. Khokonov and I. Z. Bekulova, Tech. Phys. **55**, 728 (2010).

[64] V. N. Baier, V. M. Katkov, and V. S. Fadin, *Radiation from Relativistic Electrons* (Atomizdat, Moscow, 1973).

[65] B. King, Phys. Rev. A **91**, 033415 (2015).

[66] K. Mølmer and Y. Castin, Quantum Semiclass. Opt. **8**, 49 (1996).

[67] M. B. Plenio and P. L. Knight, Rev. Mod. Phys. **70**, 101 (1998).

[68] L. H. Thomas, Nature (London) **117**, 514 (1926).

[69] L. H. Thomas, Philos. Mag. **3**, 1 (1927).

[70] V. Bargmann, L. Michel, and V. L. Telegdi, Phys. Rev. Lett. **2**, 435 (1959).

[71] M. W. Walser, D. J. Urbach, K. Z. Hatsagortsyan, S. X. Hu, and C. H. Keitel, Phys. Rev. A **65**, 043410 (2002).

[72] See Supplemental Material at http://link.aps.org/supplemental/10.1103/PhysRevLett.122.154801 for details on the employed laser fields, on the applied theoretical model, and on the simulation results for other laser or electron parameters.

[73] Y. I. Salamin and C. H. Keitel, Phys. Rev. Lett. **88**, 095005 (2002).

[74] Y. I. Salamin, G. R. Mocken, and C. H. Keitel, Phys. Rev. ST Accel. Beams **5**, 101301 (2002).

[75] E. Esarey, C. B. Schroeder, and W. P. Leemans, Rev. Mod. Phys. **81**, 1229 (2009).

[76] W. P. Leemans, A. J. Gonsalves, H.-S. Mao, K. Nakamura, C. Benedetti, C. B. Schroeder, C. Tóth, J. Daniels, D. E. Mittelberger, S. S. Bulanov, J.-L. Vay, C. G. R. Geddes, and E. Esarey, Phys. Rev. Lett. **113**, 245002 (2014).

[77] B. Gonzalez-Izquierdo, R. J. Gray, M. King, R. Wilson, R. J. Dance, H. Powell, D. A. MacLellan, J. McCreadie, N. M. H. Butler, S. Hawkes, J. S. Green, C. D. Murphy, L. C. Stockhausen, D. C. Carroll, N. Booth, G. G. Scott, M. Borghesi, D. Neely, and P. McKenna, High Power Laser Sci. Eng. **4**, e33 (2016).

[78] G. C. Rodrigues and J. R. Duflou, J. Mater. Process. Technol. **264**, 448 (2019).

[79] X. Wang *et al.*, Nat. Commun. **4**, 1988 (2013).

[80] B. Wolter, M. G. Pullen, A. T. Le, M. Baudisch, K. Doblhoff-Dier, A. Senftleben, M. Hemmer, C. D. Schroter, J. Ullrich, T. Pfeifer, R. Moshammer, S. Grafe, O. Vendrell, C. D. Lin, and J. Biegert, Science **354**, 308 (2016).

[81] R. P. Chatelain, V. R. Morrison, B. L. M. Klarenaar, and B. J. Siwick, Phys. Rev. Lett. **113**, 235502 (2014).

[82] L. D. Landau and E. M. Lifshitz, *The Classical Theory of Fields* (Elsevier, Oxford, 1975).

[83] K. Poder *et al.*, Phys. Rev. X **8**, 031004 (2018).